11 August 2000

ELSEVIER

Chemical Physics Letters 326 (2000) 58–64

CHEMICAL PHYSICS LETTERS

www.elsevier.nl/locate/cplett

Low temperature phase transition in n-pentane C_{60} clathrate: a Raman scattering study

P.M. Rafailov [a,*], V.G. Hadjiev [b], C. Thomsen [a], K. Kamarás [c], S. Pekker [c]

[a] *Institut für Festkörperphysik, Technische Universität Berlin, Hardenbergstrasse 36, D-10623 Berlin, Germany*
[b] *ISSO and Texas Center for Superconductivity Texas, University of Houston, Houston, TX 77204-5932, USA*
[c] *Research Institute for Solid State Physics of the Hungarian Academy, of Sciences, P.O. Box 49, 1525 Budapest, Hungary*

Received 10 September 1999; in final form 13 June 2000

Abstract

We present results on Raman scattering from a C_{60}.n-pentane ($C_{60}.(n\text{-}C_5H_{12})_{0.88}(C_7H_8)_{0.05}$) clathrate crystal in the range 20–300 K. The Raman intensity, in particular of the H_g modes, increases several times with lowering temperature below 160–200 K accompanied by significant reduction of the linewidths. The onset of this peculiar temperature behavior correlates with the reported phase transition in n-pentane clathrate. We argue that these findings give a Raman scattering signature for a low-temperature orientational phase transition in C_{60}.n-pentane similar to that observed for solid C_{60}. © 2000 Published by Elsevier Science B.V.

1. Introduction

The C_{60}-clathrates are fullerene-based compounds that contain a second molecular species in the crystal lattice. In clathrates, typically containing aliphatic hydrocarbons, the included molecules interact with the fullerenes via weak Van der Waals forces without charge transfer [1]. Solvates are compounds where more substantial interactions occur, examples being aromatic hydrocarbons or CS_2 [2]. However, even in clathrates, large guest molecules may cause a substantial rearrangement of the cubic structure of solid C_{60} in order to form clathrate crystals. C_{60}-clathrate crystals with orthorhombic symmetry, containing n-pentane, diethylether and dibromopropane, have been synthesized and their structure determined [3,4]. The crystal structure of C_{60}.n-pentane can be derived from that of the pristine C_{60} fullerite by appropriate shifting of planes in the cubic lattice of fullerite. In this clathrate, the C_5H_{12} molecules are packed in channels forming zig-zag arrays between adjacent C_{60} layers [3].

C_{60}-clathrate materials are interesting for they provide the opportunity to investigate quasi-isolated fullerene molecules in solids. Most of the work done so far has been focused on exploring the molecular dynamics of C_{60} and the guest molecules [5–7] and the microscopic nature of interactions between the clathrate constituents [5–8]. Pristine fullerite undergoes a first-order transition upon cooling from a face centered (*fcc*) to a simple cubic (*sc*) lattice at a temperature near 260 K [9]. In the *fcc* phase the C_{60} molecules execute quasi-free rotations about their equilibrium positions in the lattice, which are re-

* Corresponding author. Permanent address: Faculty of Physics, University of Sofia, BG-1164 Sofia, Bulgaria. Fax: +359-2-962-52-76; e-mail: rafailov@phys.uni-sofia.bg

0009-2614/00/$ - see front matter © 2000 Published by Elsevier Science B.V.
PII: S0009-2614(00)00769-7

duced in the *sc* phase to 'ratchet'-like orientational motions (librational modes) about the [111]-directions [10–12]. According to Refs. [3–5] the rotational freedom of fullerenes in C_{60}.n-pentane is preserved down to 200 K and a phase transition to an orientationally ordered phase takes place between 200 and 160 K.

The vibrational properties of the C_{60} molecule are sensitive to deformations reducing its high symmetry as has been shown for substituted C_{60} (e.g. in organo-metallic complexes like $Pt(PPh_3)_2Cl_2$ [13]) and C_{60} in solutions due to interaction with the solvent [2,14]. In addition, electronic effects, such as doping, are also known to modify vibrational spectra of C_{60} [15]. Thus it is instructive to apply vibrational spectroscopy as a complementary method for the clathrate research.

In this Letter we present a Raman study of C_{60}.n-pentane in the temperature interval 20–305 K. We also give a comparative analysis of the experimental data for C_{60}.n-pentane and pristine C_{60} fullerite.

2. Experiment

C_{60}.n-pentane clathrate crystals were grown from a saturated toluene solution of C_{60} by slow diffusion of petroleum ether, a 1:1 mixture of n-pentane and isopentane. Since C_{60} is practically insoluble in ether, crystallization occurs at the interface, the resulting clathrates containing n-pentane but no isopentane because of geometrical restrictions. Preparation details are given in Ref. [3]. Crystals of lateral dimensions 15–20 μm and 5–6 μm thickness were pressed into an indium substrate. The Raman measurements were performed on a Dilor XY 800 triple grating spectrometer with a liquid N_2 cooled CCD-detector. The Ar^+-laser line at 2.41 eV was used as an excitation source. The spectrometer slits were set to $2.5\,cm^{-1}$ spectral width and absolute accuracy of $0.5\,cm^{-1}$. The laser beam was focused to a spot of diameter ≈ 1 μm using microscope optics and the laser power was kept at 30 μW. Under these conditions line positions and sample morphology remained constant, even after long laser exposure. Raman spectra of a pure C_{60} single crystal were measured under the same conditions for reference. The low temperature measurements were made in vacuum using an Oxford micro-cryostat.

3. Results and discussion

Raman spectra of C_{60}.n-pentane clathrate taken at various temperatures are presented in Fig. 1a and 1b for the low- and the high-frequency regions, respectively. As expected for a Van der Waals bonded solid, the clathrate spectra are dominated by the strong C_{60} intramolecular modes. We have investigated in detail the two A_g modes and the six most intensive of the eight H_g modes of C_{60} in both clathrate and fullerite crystals. These modes cover the entire first-order-intramolecular spectrum and represent both radial (low frequency) and tangential (high frequency) type vibrations. The Raman spectra of both samples at 20 and 305 K are compared in Fig. 2. The lines that correspond to Raman forbidden modes in isolated C_{60} are assigned according to Refs. [1,16].

The temperature dependence of the relative peak intensity (spectral weight under the peak), normalized to the corresponding peak intensity at 305 K, for each mode in both samples is plotted in Fig. 3. Fig. 4 displays the temperature dependence of the linewidths. We can summarizene the experimental observations dividing the examined temperature interval into two regions:

(i) From 305 K to approximately 200 K the Raman intensity of the clathrate sample remains relatively unchanged in contrast to pure C_{60} with intensities growing rapidly below 260 K. Most H_g lines of C_{60}.n-pentane appear as broad features with full width at half maximum (FWHM) ranging from $7\,cm^{-1}$ to over $15\,cm^{-1}$, the only exception being the $H_g(1)$ mode with a FWHM $\approx 4\,cm^{-1}$. The two A_g lines of both samples have widths about $2–4\,cm^{-1}$ that remain nearly unchanged for all temperatures probed by our measurements. The H_g lines of the pure C_{60} crystal exhibit a similar broadening in the 'rotational disorder'-phase above 260 K [17,18].

(ii) Below ≈ 200 K the intensities of all peaks of the clathrate sample increase several times (Fig. 3) with respect to their values at 305 K. This is accom-

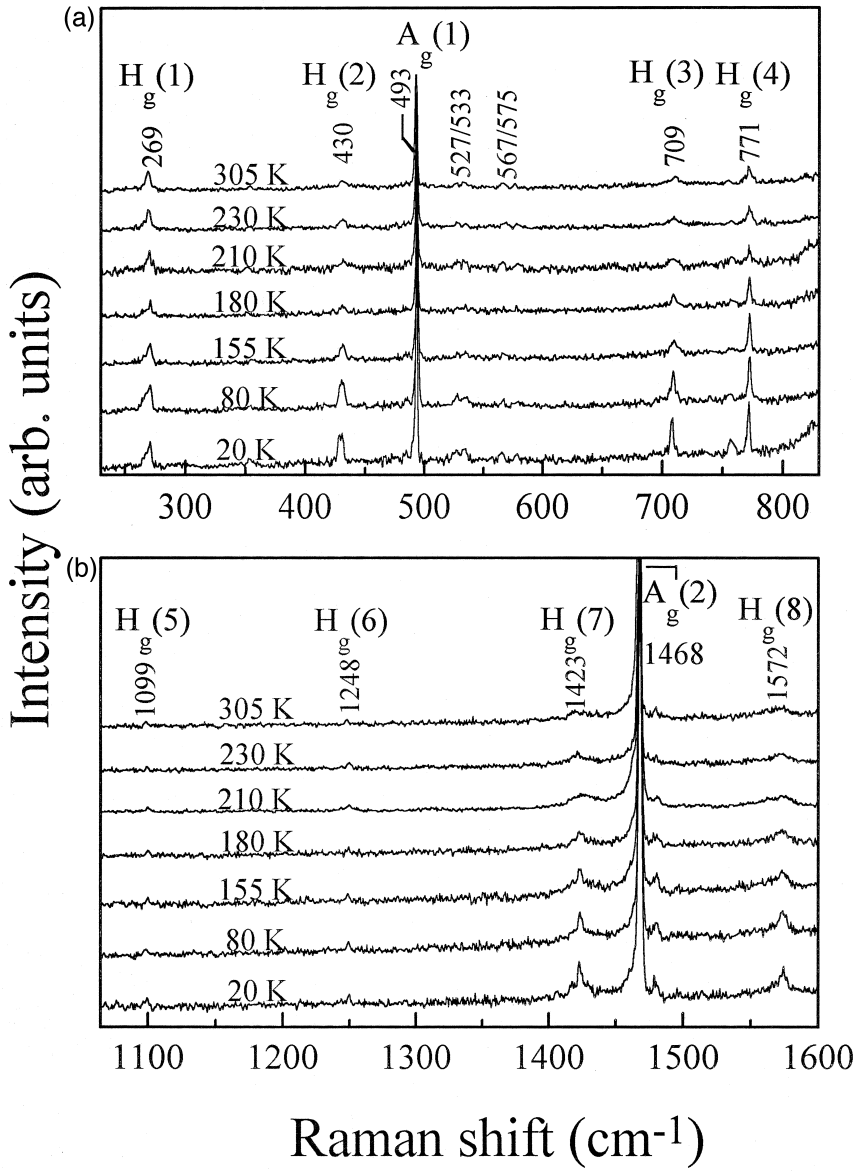

Fig. 1. The Raman spectra of a C_{60}.n-pentane crystal given for seven elevated temperatures: (a) low frequency (radial type) modes; (b) high frequency (tangential type) modes.

panied by a narrowing of the H_g-linewidths to values between $3\,cm^{-1}$ ($H_g(4)$) and $7\,cm^{-1}$ ($H_g(8)$) (see Fig. 4).

We begin our analysis of the high-temperature phase of C_{60}.n-pentane by recalling recent X-ray diffraction studies and molecular dynamics simulations [5]. The results of Ref. [5] suggest that C_{60} in C_{60}.n-pentane rotates freely and C_2H_5 molecules execute flip-flop-like motions between two symmetry related positions for temperatures above 160 K. The line broadening in the higher temperature Raman spectra in Fig. 1 provides further evidence for the C_{60} rotation. A strong coupling to the motion of C_2H_5 which would cause the broadening (instead of

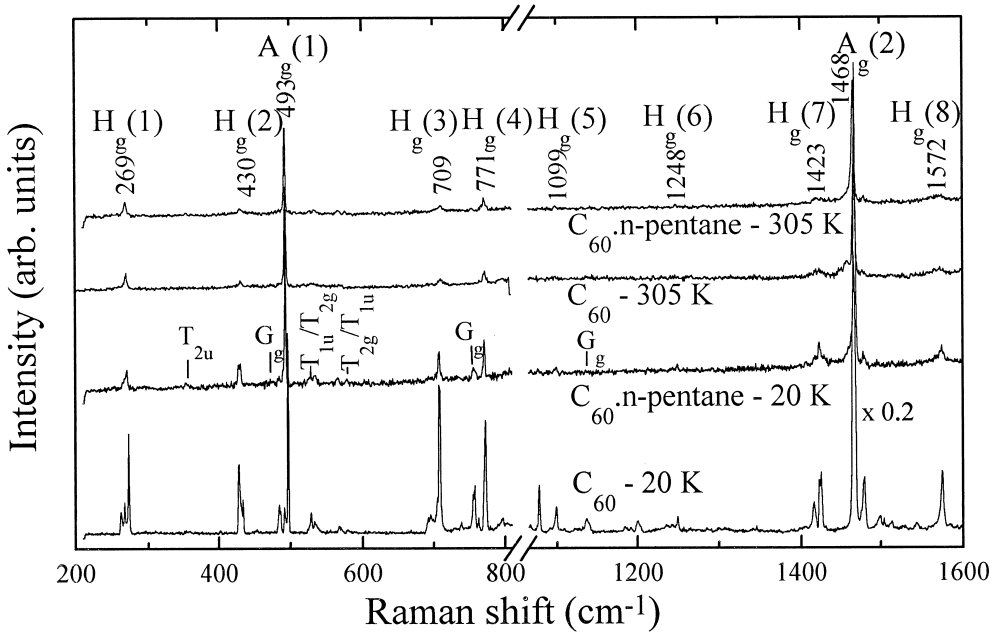

Fig. 2. Comparative view of the Raman spectra of C_{60}.n-pentane and pristine C_{60} at 20 K and 305 K.

C_{60} rotation) is not likely in view of the weak bonding between host and guest molecules. Nevertheless, the rotational freedom of C_{60} in clathrates seems to be slightly modified when compared with

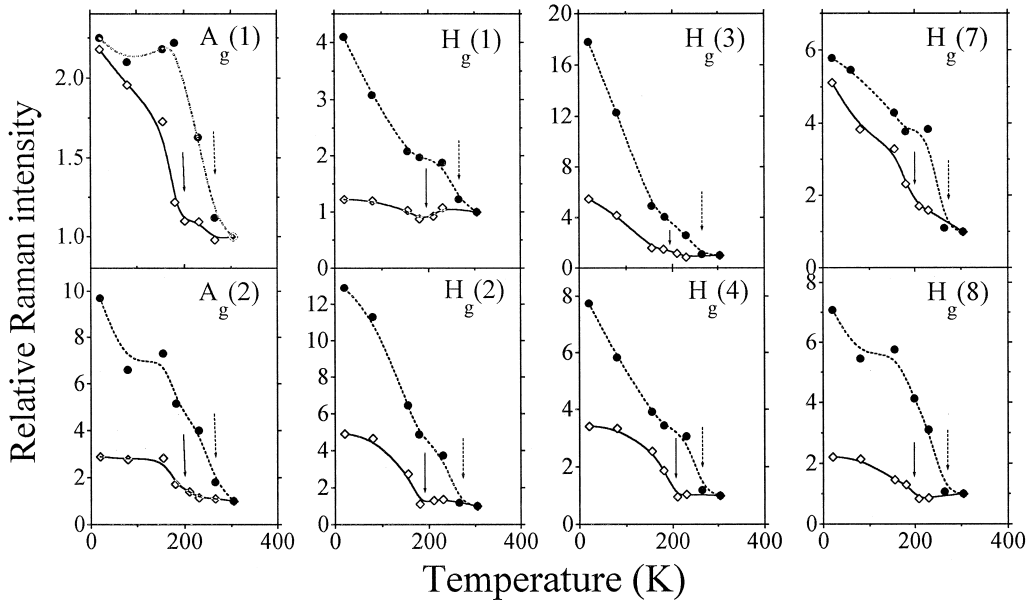

Fig. 3. Relative peak intensities (normalized to the values at 305 K) vs temperature of a C_{60}.n-pentane clathrate(diamonds) and a pure C_{60} crystal (circles). The connecting lines are guides to the eye.

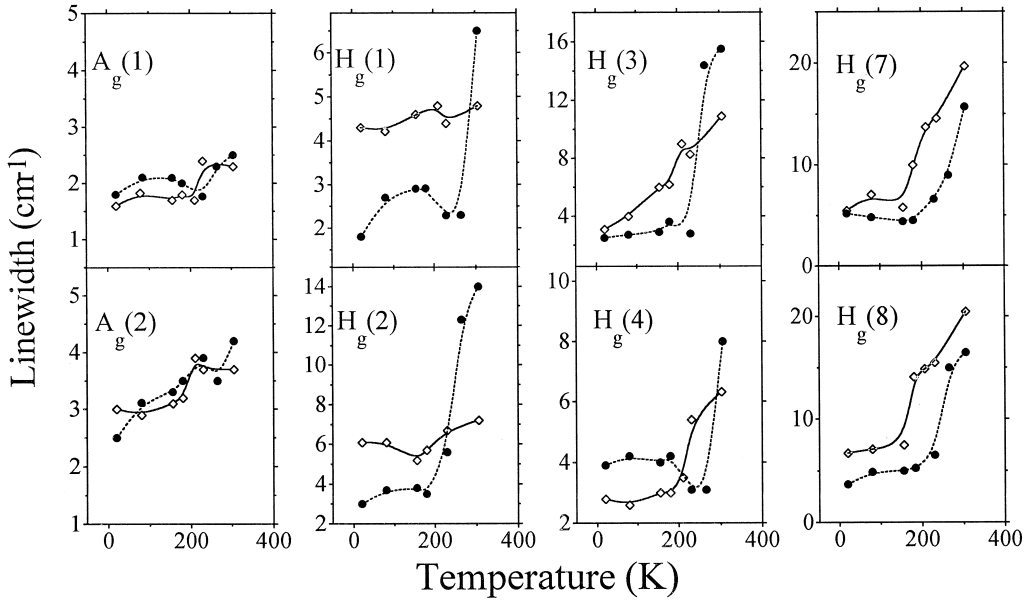

Fig. 4. Temperature dependence of the linewidths of the Raman active modes in C_{60}.n-pentane clathrate (diamonds) and pure C_{60} (circles). The connecting lines are guides to the eye.

pristine C_{60} as indicated by the different broadening of the H_g lines.

At room temperature C_{60}.n-pentane has a face-centered orthorhombic unit cell (space group $Ama2_1$) [3]. The point group C_{2v} of the clathrate lattice possesses no inversion symmetry and C_{60} occupies two sites of C_s symmetry per primitive cell [19]. Due to the clathrate crystal field, the low-lying (between 2 and 3 eV) T_{2u}, G_u and H_u electronic states in the C_{60} molecule, that take part in only dipole-forbidden transitions from the ^1A_g ground state [20,21], are expected to split according to the symmetry descent $I_h \rightarrow C_{2v} \rightarrow C_s$:

$$T_{2u}/T_{1u} \rightarrow 2A_1 + A_2 + B_1 + 2B_2,$$

$$G_u \rightarrow 2A_1 + 2A_2 + 2B_1 + 2B_2,$$

$$H_u \rightarrow 2A_1 + 3A_2 + 3B_1 + 2B_2. \quad (1)$$

Since the dipole operator, that has T_{1u} symmetry for the I_h group, contains A_1, B_1 and B_2 symmetry components in C_{2v}, several electronic transitions around the laser excitation at 2.41 eV become dipole-allowed. On the other hand, the chaotic rotation of C_{60} at high temperatures in clathrates is expected to smear out the crystal field effects similarly to the case of pristine C_{60} [22]. Therefore, the Raman scattering from C_{60}.n-pentane at temperatures above 200 K is near a resonance with the 2.41 eV excitation that is somewhat diminished by the rotational motion.

The strong change in Raman intensities and lineshapes of C_{60}.n-pentane below ≈ 200 K closely resembles that for pristine C_{60} below 260 K. The latter has been related to the orientational ordering of solid C_{60} at low temperatures [22]. By analogy, we attribute the Raman lines changes in C_{60}.n-pentane to the orientational ordering of the buckyballs below 200 K [4]. Precise X-ray measurements of the phase transition in C_{60}.n-pentane implied that the change of the lattice parameters occurs step-like upon decreasing the temperature below 200 K, and a monoclinic structure is established at about 160 K [6]. This structure, however, can be regarded as a slight modification of the orthorhombic lattice and can be derived from the latter by small changes of $\approx 1°$ of the unit cell angles [6]. Therefore, the dipole-allowed transitions given by Eq. (1) are also relevant to the oientationally ordered state.

In Albrecht's treatment of Raman intensity [23,24], the Raman scattering from the totally symmetric

$A_g(1)$ and $A_g(2)$ modes is mainly governed by the Franck–Condon term (A-term). It gives resonant enhancement only for laser excitations close to dipole-allowed transitions. The Herzberg–Teller term (B-term) contributes to the intensity of predominantly non-totally symmetric Raman active modes. It leads to a stronger resonance because it contains the vibronic coupling of the resonant electronic state to other near-lying states [23]. While A_g modes can couple only dipole-allowed states, the H_g modes (or their non-totally symmetric split components) can couple all odd parity states to the resonant state [24]. The H_g-derived vibrations may thus gain intensity from the Herzberg–Teller coupling of forbidden and allowed states. This may be the reason for their stronger enhancement in the orientationally ordered phase as compared to the A_g modes (Fig. 3).

The crystal field splitting of the dipole-forbidden electronic states of C_{60} in the ordered phase is essential for the effectiveness of the Herzberg–Teller coupling because the energy interval between these states is in principle larger than the highest vibrational energy. The splitting of the phonon lines $A_g \rightarrow A_1 + B_2$ and $H_g \rightarrow 3A_1 + 2A_2 + 3B_1 + 2B_2$ at low temperatures (see Fig. 2) also reflects the crystal field strength. In Table 1 we present the measured splitting $\delta\omega$ of the $A_g(1)$, $H_g(1)$, $H_g(2)$ and $H_g(7)$ lines at 20 K. We exclude the $H_g(3)$-line whose low frequency shoulder was assigned to the $H_g(1) + H_g(2)$ combination mode [25]. The splitting of the remaining lines, if any, is not well resolved. As follows from Table 1, the splitting of vibrational modes in pure fullerite is about twice as large as in C_{60}-n-pentane and a similar effect should be expected for the electronic states. On the other hand, the increase of Raman intensity with lowering temperature in pure fullerite exceeds that in C_{60}-n-pentane by a factor of 2–3 (Fig. 3). Therefore, the strength of the Raman resonance correlates with the splitting which, in turn, depends on the crystal field. Additional evidence for a weaker strength of the crystal field in the n-pentane clathrate is the observed blue shift of the optical absorption edge with respect to that of pure C_{60} which indicates a reduced overlap of adjacent C_{60} orbitals [26].

Table 1
Average splitting $\delta\omega$ (in cm^{-1}) at 20 K of the lines $A_g(1)$, $H_g(1)$, $H_g(2)$ and $H_g(7)$ in the Raman spectra of pure C_{60} and C_{60}.n-pentane

Sample	$A_g(1)$	$H_g(1)$	$H_g(2)$	$H_g(7)$
pure C_{60}	5	5.5	6	8
C_{60}.n-pentane	2	3	3.5	5.5

Due to the weak (Van der Waals) intermolecular interaction the features that are derived from the Raman-allowed modes in icosahedral C_{60} are dominant in the spectra of both samples at all temperatures (Figs. 1 and 2). Nevertheless, the difference in the crystal symmetry becomes also evident from the weak new modes that appear in the Raman spectra at low temperatures. In pure fullerite, these are mostly even-parity modes (T_{1g}, T_{2g} and G_g) that become active due to the cubic symmetry of the crystal lattice [16]. In $C_{60} \cdot$ n-pentane, however, the odd-parity modes are more strongly enhanced. For instance, the intensity ratio at 20 K of the $G_g(1)$-line at 485 cm^{-1} and the T_{1u}-line at 527 cm^{-1} (see Fig. 2) is 1.5 for pure fullerite and 0.4 for $C_{60} \cdot$ n-pentane. Proliferation of IR-active or silent modes due to charge transfer like in electron-donating solvents [14,24] is not likely to occur in the n-pentane crystal. The stronger relative enhancement of odd-parity modes below the phase transition is an indication for the essentially non-centrosymmetric properties of the crystal field in $C_{60} \cdot$ n-pentane. In the low temperature sc-phase of pure C_{60} the inversion symmetry is largely preserved in spite of the incompatibility of the icosahedral with the cubic symmetry and the disorder effects that allow for the activation of forbidden modes in the Raman spectra [16,24,27].

4. Conclusions

In summary, we have presented Raman scattering evidence that C_{60} molecules in $C_{60} \cdot$ n-pentane rotate at room temperature and the orthorhombic crystal symmetry has only a weak influence on them. Below 200 K, the interaction between the molecules in the crystal increases and results in orientational ordering and strengthening of the electron–phonon interaction. This leads to an enhancement of the scattering intensity and also to a splitting and the appearance of new Raman lines. The simultaneous cancelling of the free rotation causes a general narrowing of the Ra-

man lines. The presence of the guest molecules weakens the resonance intensity enhancement in comparison to pristine C_{60}. The results confirm the presence of a low temperature phase transition in $C_{60} \cdot$ n-pentane that corresponds to the *fcc* to *sc* transition in pristine C_{60} solids.

Acknowledgements

We thank H. Jantoljak for helping with the measurements. P.M.R. acknowledges a research fellowship from the Deutscher Akademischer Austauschdienst. This work was supported in part by Contract OTKA T019139 of the Hungarian National Research Foundation.

References

[1] M.S. Dresselhaus, G. Dresselhaus, P.C. Eklund, Science of Fullerenes and Carbon Nanotubes, Academic Press, New York, 1996.
[2] S.H. Gallagher, R.S. Armstrong, P.A. Lay, C.A. Reed, J. Phys. Chem. 99 (1995) 5817.
[3] S. Pekker, G. Faigel, K. Fodor-Csorba, L. Granasy, E. Jakab, M. Tegze, Solid State Comm. 83 (1992) 423.
[4] S. Pekker, G. Faigel, G. Oszlanyi, M. Tegze, T. Kemeny, E. Jakab, Synth. Metals 55/57 (1993) 3014.
[5] G. Oszlanyi, G. Bortel, G. Faigel, S. Pekker, M. Tegze, Solid State Comm. 89 (1994) 417.
[6] G. Faigel, G. Bortel, G. Oszlanyi, S. Pekker, M. Tegze, Phys. Rev. B 49 (1994) 9186.
[7] V.N. Semkin, N.G. Spitsina, A. Graja, Chem. Phys. Lett. 233 (1995) 291.
[8] V.N. Semkin, N.V. Drichko, Yu.A. Kumzerov, D.V. Konarev, R.N. Lyubovskaya, A. Graja, Chem. Phys. Lett. 295 (1998) 266.
[9] P.A. Heiney, J.E. Fisher, A.E. McGhie, W.J. Romanow, A.M. Denenstein, J.P. McCauley Jr., A.B. Smith III, D.E. Cox, Phys. Rev. Lett. 66 (1991) 2911.
[10] R. Tycko, G. Dabbagh, R.M. Fleming, R.C. Haddon, A.V. Makhija, S.M. Zahurak, Phys. Rev. Lett. 67 (1991) 1886.
[11] R. Sachidanandam, A.B. Harris, Phys. Rev. Lett. 67 (1991) 1467.
[12] W.I.F. David, R.M. Ibberson, J.C. Matthewman, K. Prassides, T.J.S. Dennis, J.P. Hare, H.W. Kroto, R. Taylor, D.R.M. Walton, Nature (London) 353 (1991) 147.
[13] B. Chase, P. Fagan, J. Am. Chem. Soc. 114 (1992) 2252.
[14] S.H. Gallagher, R.S. Armstrong, P.A. Lay, C.A. Reed, Chem. Phys. Lett. 248 (1996) 353.
[15] M.G. Mitch, S.J. Chase, J.S. Lannin, Phys. Rev. Lett. 68 (1992) 883.
[16] P.H.M. van Loosdrecht, P.J.M. van Bentum, M.A. Verheijen, G. Meijer, Chem. Phys. Lett. 198 (1992) 587.
[17] P.H.M. van Loosdrecht, P.J.M. van Bentum, G. Meijer, Phys. Rev. Lett. 68 (1992) 1176.
[18] B. Burger, H. Kuzmany, Electronic Properties of Novel Materials, World Scientific, London, 1994.
[19] K. Kamarás, V.G. Hadjiev, C. Thomsen, S. Pekker, K. Fodor-Csorba, G. Faigel, M. Tegze, Chem. Phys. Lett. 202 (1993) 325.
[20] S. Leach, M. Vervloet, A. Després, E. Bréheret, J.P. Hare, T.J. Dennis, H.W. Kroto, R. Taylor, D.R.M. Walton, Chem. Phys. 160 (1992) 451.
[21] F. Negri, G. Orlandi, F. Zerbetto, Chem. Phys. Lett. 144 (1992) 31.
[22] V.G. Hadjiev, P.M. Rafailov, H. Jantoljak, C. Thomsen, M.K. Kelly, Phys. Rev. B 56 (1997) 2495.
[23] A.C. Albrecht, J. Chem. Phys. 34 (1961) 1476.
[24] S.H. Gallagher, R.S. Armstrong, W.A. Clucas, P.A. Lay, C.A. Reed, J. Phys. Chem. 101 (1997) 2960.
[25] P.J. Horoyski, M.L.W. Thewalt, T.R. Anthony, Phys. Rev. B 54 (1996) 920.
[26] K. Kamarás, A. Breitschwerdt, S. Pekker, K. Fodor-Csorba, G. Faigel, M. Tegze, Appl. Phys. A 56 (1993) 231.
[27] P. Bowmar, W. Hayes, M. Kurmoo, P.A. Pattenden, M.A. Green, P. Day, K. Kikuchi, J. Phys.: Condensed Matter 6 (1994) 3161.